Nanoscale Res Lett (2009) 4:437–443
DOI 10.1007/s11671-009-9265-2

NANO EXPRESS

CdSe Ring- and Tribulus-Shaped Nanocrystals: Controlled Synthesis, Growth Mechanism, and Photoluminescence Properties

Pengfei Hu · Dianzeng Jia · Yali Cao · Yudai Huang · Lang Liu · Jianmin Luo

Received: 24 November 2008 / Accepted: 27 January 2009 / Published online: 18 February 2009

Abstract With air-stable and generic reagents, CdSe nanocrystals with tunable morphologies were prepared by controlling the temperature in the solution reaction route. Thereinto, the lower reaction temperature facilitates the anisotropic growth of crystals to obtain high-yield CdSe ring- and tribulus-shaped nanocrystals with many branches on their surfaces. The photoluminescence properties are sensitive to the nature of particle and its surface. The products synthesized at room temperature, whose surfaces have many branches, show higher blue shift and narrower emission linewidths (FWHM) of photoluminescence than that of samples prepared at higher temperature, whose surfaces have no branches. Microstructural studies revealed that the products formed through self-assembly of primary crystallites. Nanorings formed through the nonlinear attachment of primary crystallites, and the branches on the surfaces grew by linear attachment at room temperature. And the structure of tribulus-shaped nanoparticle was realized via two steps of aggregation, i.e., random and linear oriented aggregation. Along with the elevation of temperature, the branches on nanocrystal surfaces shortened gradually because of the weakened linear attachment.

Keywords CdSe nanostructure · Tunable morphologies · Narrow emission linewidth · Nonlinear and linear attachment · Two-step attachment

Introduction

Cadmium selenide (CdSe), one of the important II–VI group semiconductors, has received significant interest in the field of optoelectronic applications due to its broad range of optical transmissions, excellent nonlinear optical properties, and quantum size effects [1–6]. For these applications, the efficiency and line width of the photoluminescence (PL) are important factors. And these PL properties are very sensitive to the nature of the particle and its surface [3]. Up to now, shape-controlled synthesis of CdSe nanorods [7–13], nanowires [14–17], nanotubes [18], nanobelts [15, 19], nanosaws [15], nanobarbells [20], and many novel nanostructures [21–24] have been demonstrated. The popular routes to synthesize CdSe, whether the west coast method (TBP/TOPO) or the east coast method (TOP/TOPO), generally require rather complicated procedures including delicate control of surfactant ratios and inert reaction conditions due to the toxic and unstable nature of the precursors [25]. So, with the exploration of the electrical and photoluminescence properties of the nano-sized CdSe, a convenient and effective synthetic method is still a focus for researchers. Concerning the unique structural features and better properties generated with them, the nonlithographic fabrication of free-standing CdSe nanorings (strict circular, oval, homocentric, or polygonal forms) and other novel nanostructure objects from small building blocks by self-organizing means may represent a next challenge of nanofabrication.

Electronic supplementary material The online version of this article (doi:10.1007/s11671-009-9265-2) contains supplementary material, which is available to authorized users.

P. Hu · D. Jia (✉) · Y. Cao · Y. Huang · L. Liu
Institute of Applied Chemistry, Xinjiang University, Urumqi 830046, People's Republic of China
e-mail: jdz@xju.edu.cn

J. Luo
Physics and Chemistry Test Centre, Xinjiang University, Urumqi 830046, People's Republic of China

In view of the advantages of the solution reaction route, low energy consumption, and facility, we introduce it to explore a general synthetic method for CdSe nanomaterials at low temperature. In this work, we successfully developed a low temperature and convenient solution reaction approach to fabricate CdSe nanocrystals. This method does not require complex apparatus, expensive reagents, or complicated techniques. It can synthesize CdSe nanomaterials with branches on surface in high-yield. Shape control was achieved by varying the reaction temperature conveniently and it does not need any organic additives. Based on the self-assembly of nanocrystals, the formation mechanism of nanorings and tribulus-shaped nanoparticles were discussed in detail. Furthermore, the photoluminescence properties were investigated.

Experimental Section

All the reagents were of analytical-grade and were used without further purification. The synthesis of sample **I** was carried out through solution reaction process. Firstly, the selenium powder (Se) was put into the hydrazine hydrate ($N_2H_4 \cdot H_2O$) in a three-necked flask under magnetic

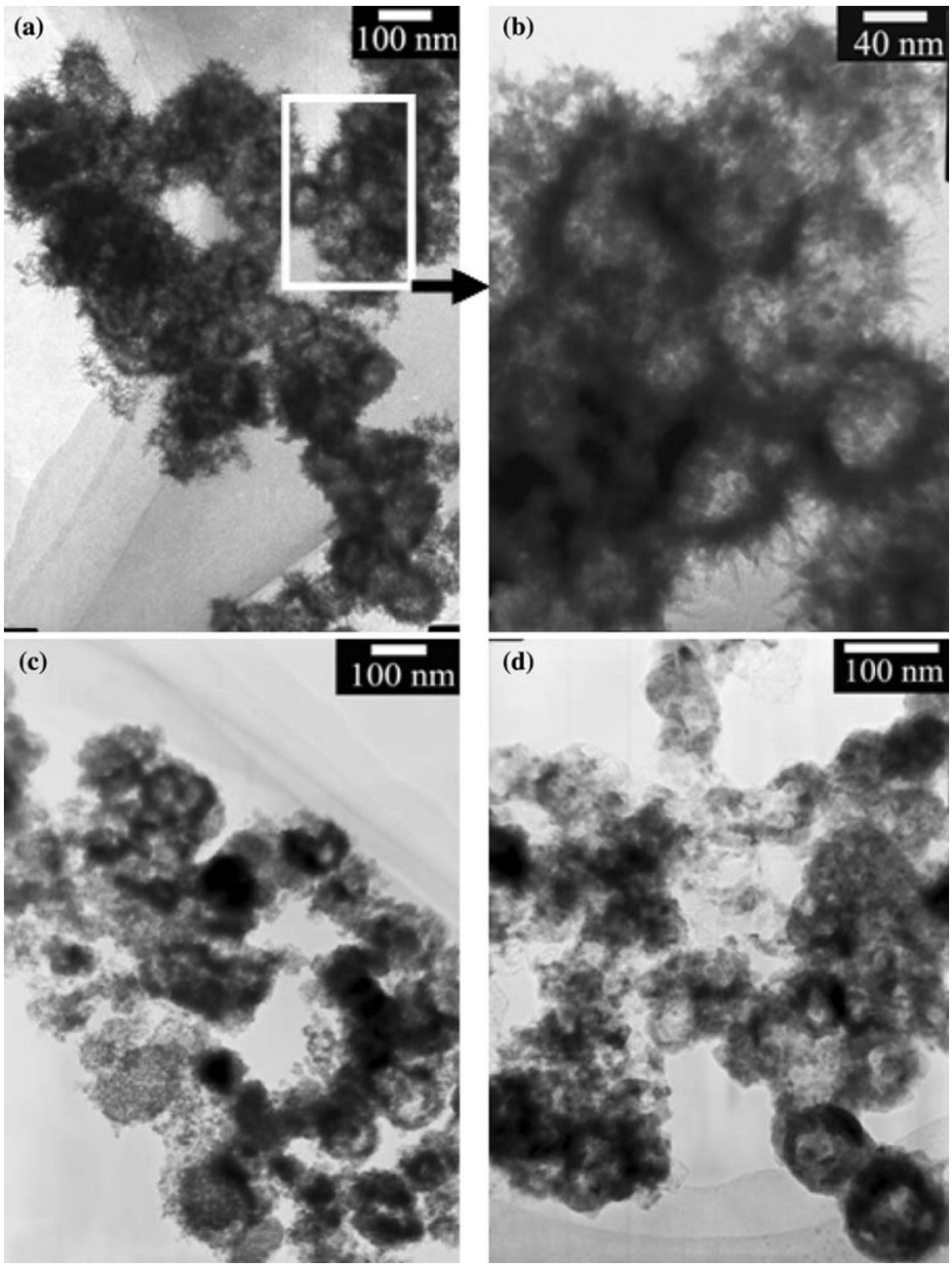

Fig. 1 Typical TEM images of CdSe nanocrystals synthesized at **a** and **b** room temperature (sample **I**), **c** 60 °C (sample **II**), and **d** 100 °C (sample **III**)

stirring. The process was carried out at room temperature till a resultant brown solution was got. Subsequently, the $Cd(CH_3COO)_2 \cdot 2H_2O$ (the molar ratio of Cd^{2+}:Se = 2:1) was added to the above solution and stirred for 2 h. The products were filtered and washed with distilled water and ethanol for five times, respectively. Finally, the orange product powder was dried at 60 °C for 4 h in air oven and collected for further characterization. Sample **II** and **III** were synthesized at 60 °C and 100 °C, respectively and other experimental parameters are consistent. Worth the whistle, all processes were carried out in fume cupboard.

Powder X-ray diffraction (XRD, MXP18AHF, MAC) using Cu$K\alpha$ radiation ($\lambda = 0.154056$ nm) was adopted to identify the crystalline phase of the resulting materials. Transmission electron microscopic analysis (TEM) and high-resolution transmission electron microscopic analysis (HRTEM) were performed with HITACHI H-600 (TEM, HITACHI H-600) microscope operating at 75 kV and a JEOL JEM-2100 (TEM, JEOL JEM-2100) electron microscope operating at 200 kV, respectively. The photoluminescence spectra were obtained by using a HITACHI F-4500 fluorescence spectrophotometer at room temperature.

Results and Discussion

The TEM images demonstrated the high-yield of nanostructure with branches obtained at room temperature and structural evolution along the temperature. As shown in Figs. 1a and S1, the products synthesized at room temperature are dominated by CdSe tribulus-shaped nanoparticles and nanorings. Figure 1b and the magnified images of Figs. 1a and S1 clearly display the branched structure on the surfaces of nanostructure. The ring-like objects involving circular, hexagonal, and oval forms, with growing outward radial thorn-like branches were exhibited in the Figs. 1a, b, 2a and S2a_1–a_7. Among them, the hexagonal rings are less populated (Fig. S2a_7). Meanwhile, there is a portion of CdSe homocentric nanorings (Fig. 2a). Enlarged images show that some rings are half-penetrated because of the attachment of the primary particles in the cavities (Figs. 2a and S2a_2, a_3, a_6). Furthermore, a series of tribulus-shaped nanocrystals were created at room temperature (Figs. 2c, 5a, c, S1 and S2b). The tribulus-shaped nanocrystals have about 3–10 cuspidal arms. These arms are 10–30 nm in length and the cusp of these arms are 3–5 nm in diameters (Figs. 3, 5a and c).

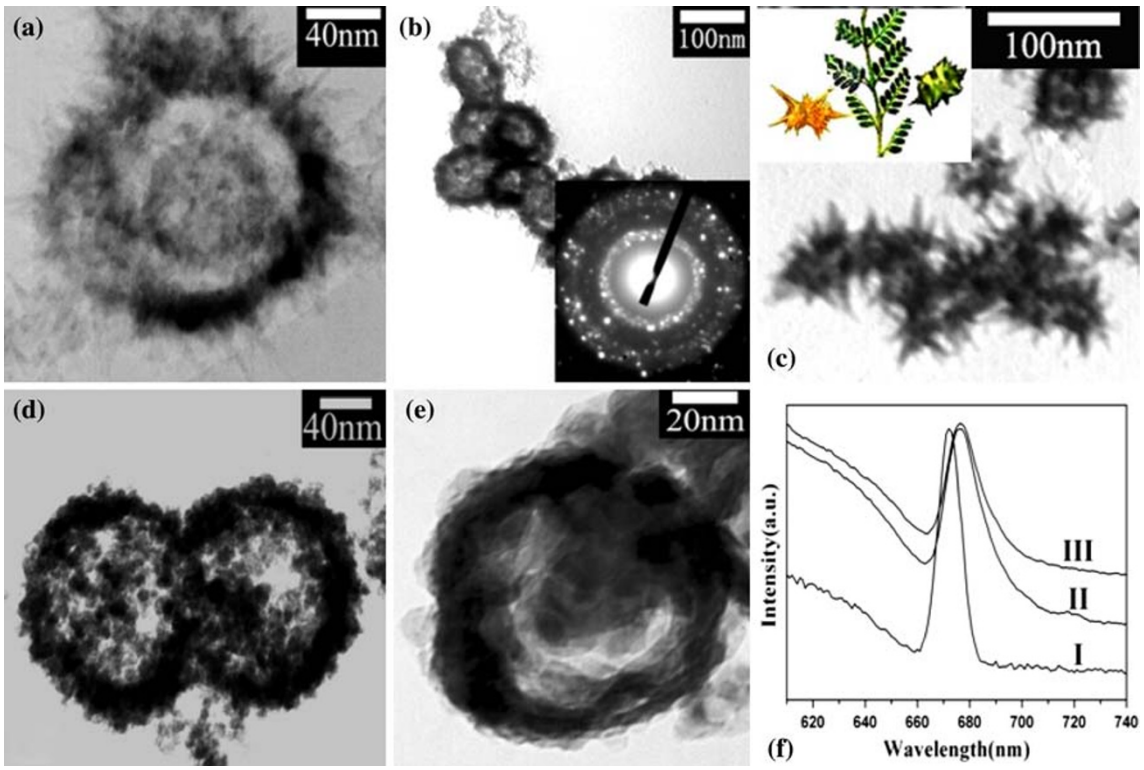

Fig. 2 **a–c** TEM Images and SAED pattern of CdSe nanocrystals synthesized at room temperature: **a** the homocentric ring; **b** the oval and irregular rings (inset is the SAED pattern of the ring in the image **b**); **c** the tribulus-shaped nanoparticles (inset is a natural tribulus); **d** and **e** TEM images of CdSe nanorings prepared at 60 °C and 100 °C, respectively; **f** Room temperature photoluminescence spectra of products obtained at (**I**) room temperature, (**II**) 60 °C, and (**III**) 100 °C (Excitation wavelength: 450 nm)

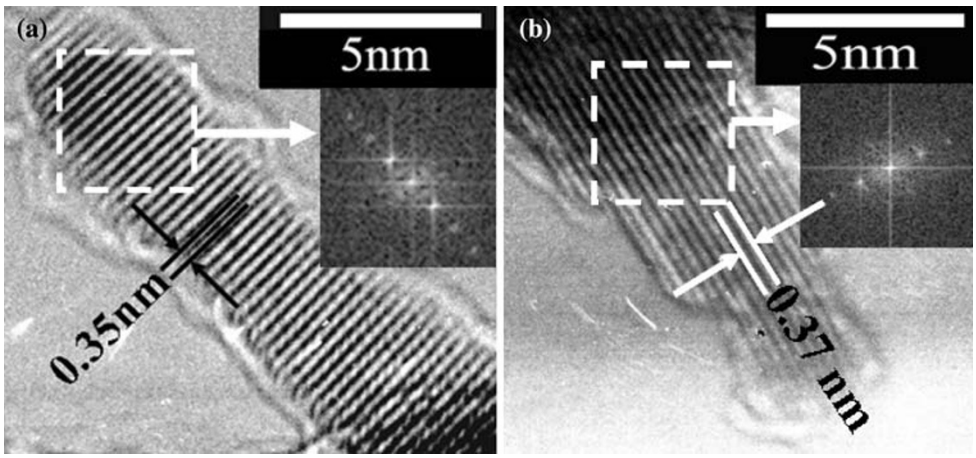

Fig. 3 The high-resolution TEM images of CdSe branches of nanocrystals synthesized at room temperature: **a** the space between arrowheads corresponds to the distance between two (0002) planes; **b** the interplanar spacing corresponds to the distance between two (10-10) planes; The inset of (**a**) and (**b**) show the FFT analysis of selective region in the crystal, respectively

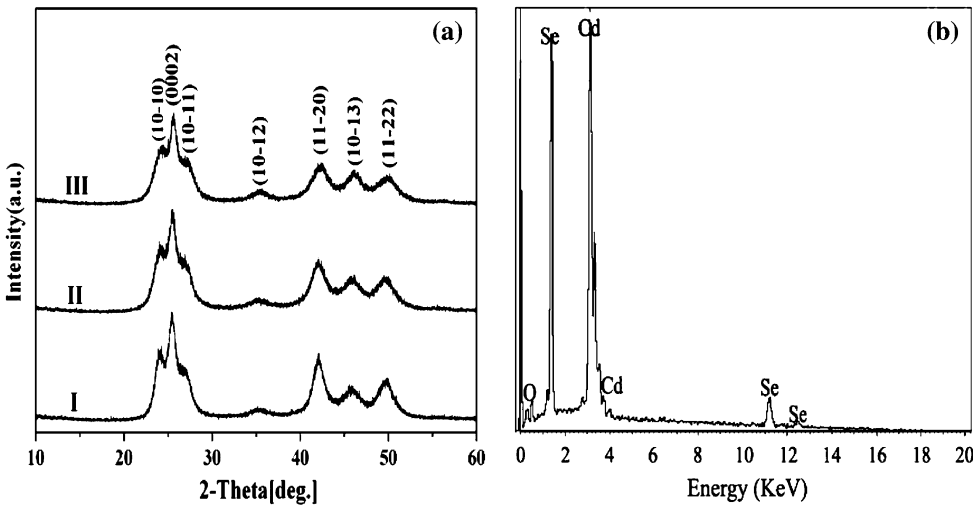

Fig. 4 **a** XRD patterns of sample **I**, **II**, and **III**; **b** EDX spectrum of CdSe sample produced at room temperature (sample **I**)

The morphology of the products varies upon the reaction temperature. The thorn-like branches of nanoparticles and nanorings obviously shortened at 60 °C and completely disappeared at 100 °C (Fig. 1c and d). In fact, the branches have become small protuberances at 60 °C (Fig. 2d). The reason for the shortening of branches on nanocrystals prepared at higher temperature will be discussed in detail at the latter paragraph. Furthermore, the yield of rings decreases while the temperature steps up. According to the statistic, the average yield of rings is about nine per TEM image in sample **I** and three in sample **II,** and two in sample **III** (based on a total of 20 TEM images of sample **I**, **II**, and **III**, respectively).

As mentioned in the introduction segment, the PL properties of the materials are very sensitive to the nature of the particle and its surface. Figure 2f compares the room temperature PL spectra of three samples in this paper. They all exhibit a strong fluorescence emission band with the similar profile centered at 672 nm (**I**), 676 nm (**II**), and 677 nm (**III**), respectively. Each as-prepared CdSe nanocrystal has a blue shift in the PL spectra, in comparison with that of bulk CdSe at 730 nm. The Full-Width-at-Half-Maximum (FWHM) is an important parameter of photoluminescence properties, which reveals the crystallinity and size distribution of nanostructure. It is the distance between two sides of a peak measured at half the peak height. The FWHM of the sample **I** fabricated at room temperature is about 13 nm, which agrees well with the higher crystallinity, and that of samples **II** and **III** are about 18 nm and 20 nm, respectively. In a word, the PL spectra demonstrate that the sample **I** prepared at room temperature has a stronger blue shift and a narrower FWHM than the samples **II** and **III** synthesized at 60 °C and 100 °C. The novel surface structure of as-obtained particles formed at room temperature may be a reason for this result. Furthermore, from the emission spectra, the size of CdSe nanoparticles which made up the polycrystalline walls of the rings or tribulus-shaped crystals was estimated to be around 10 nm in the sample **I**.

High-resolution TEM (HRTEM) shows that the arms of tribulus-shaped nanocrystals and radial branches of nanorings are well crystalline. Among them, the branches/arms

that grow along the [0001] direction are more populated. The interplanar spacing in the branches/arms is 0.35 nm which matches well with the (0002) plane of CdSe (Fig. 3a). Moreover, the (10-10) plane of CdSe can also be observed in the sample (Fig. 3b). A fast Fourier transform (FFT) analysis of the branches/arms (see inset of Figs. 3a and b) confirmed that the thorn-like branches were strictly oriented. Both the HRTEM result and FFT patterns analyses demonstrate that these thorn-like branches have <0001> or <11-20> preferential growth direction.

The X-ray diffraction (XRD) patterns show that the CdSe nanocrystals have hexagonal wurtzite structure with the diffraction peaks which shift to higher angles (Fig. 4a). The extremely sharp (0002) peak reveals the preferred <0001> orientation of the CdSe nanocrystallites. The cell constants were calculated to be $a = b = 0.4256$ nm and $c = 0.6977$ nm from (10-10) and (0002) peaks of (**I**) (sample **I**) after refinement. They revealed that the lattice contractions of $\Delta a = 1.00\%$ and $\Delta c = 0.47\%$ occurred against the reported data ($a = b = 0.4299$ nm and $c = 0.7010$ nm). A spectrum of energy-dispersive X-ray spectroscopy (EDX) for the sample **I** confirms that the atomic ratio for Cd:Se is approximately 1.13:1. And the sample contains a little oxygen element (Fig. 4b).

According to the above experimental results, we suggest the formation mechanism of nanorings and tribulus-shaped nanoparticles as follows.

For the present synthetic route, $N_2H_4 \cdot H_2O$ is used as the reducing agent (N_2/N_2H_4, OH^-, -1.15 V) and the selenium powder was reduced from zero valence to -2 valence. After this course, the as-reduced Se^{2-} reacts with Cd^{2+} to generate orange CdSe.

Our experimental results revealed that the resultant nanostructures came into being through the self-assembly of primary particles. It is well-known that the main driving force for aggregation of nanoparticles can be generally attributed to the tendency for reducing the high surface energy through the attachment among the primary nanoparticles and the formation of coherent lattice structure at grain interfaces [26–29]. The aggregation of nanoparticles contains the linear alignment which can be achieved by sharing a common crystallographic orientation among the primary particles and the nonlinear arrangement which can be attained with the lateral lattice fusion of the primary particles [30]. Generally, the linear alignment can lead to the formation of one-dimensional nanostructures (nanorods or nanowires) mostly. The nonlinear arrangement which can result in the ring-like structure has been demonstrated in the literatures [30, 31]. Literature [30] described three types of CdS nanorings which were based on the statistical assembly or specific crystallographic requirement of the tiny CdS hexagons. The rectangular PbSe nanorings resulted from the dipole-induced orientational attachment of cubic primary PbSe nanoparticles in the literature [31].

Similar to the formation of CdS nanorings [30], the first type (i) of organization of CdSe nanorings was achieved by the attachments among neighboring hexagonal building units with their {10-10} and {0001} family planes on their external surfaces. Sixfold symmetry of wurtzite CdSe {0001} surfaces make hexagonal building units having six equal chances to attach to their neighboring crystallites, and a statistical assembly of the tiny hexagons may lead to the formation of a curvature. In order to ensure a smooth curvature development, building segments of {10-10} and {11-20} should be connected in an alternative manner. Otherwise, the aggregation process will run out of a circumferential track, and the tortile and incomplete circular ring structures will be formed (Fig. 2b). The study on

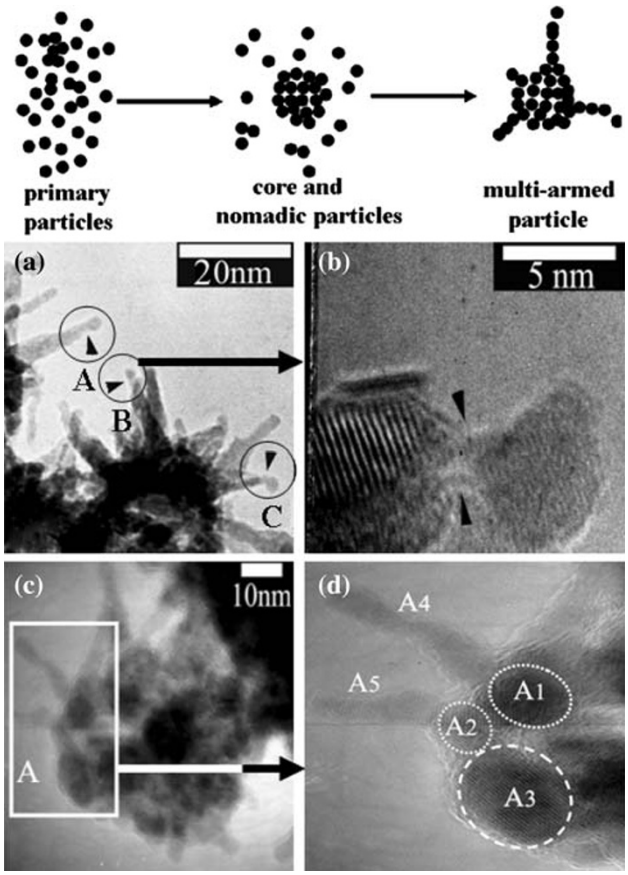

Fig. 5 Top: Schematic illustration depicted the two steps of growth based on self-assembly from primary particles to a tribulus-shaped crystal. **a** TEM image showing attachment of new particles to elongate the branches (arrowheads in the section A, B and C); **b** HRTEM image of section B in (**a**) indicating the connecting region (between arrowheads) between a new particle and the arm; **c** high-resolution TEM image of a tribulus-shaped nanoparticle; **d** magnification of the section A in (**c**) exhibiting three random arrangement particles A1, A2, A3 and two oriented attachment branches A4 (<11-20> direction) and A5 (<0001> direction)

selected area electron diffraction (SAED) in the inset of Fig. 2b reveals the polycrystalline nature for the CdSe rings.

Apart from the horizontal ring formation with the {10-10} family facets, some CdSe primary nanocrystallites can also stack along the <0001> axis, where the *c*-plane terminates either with positively charged (0001)-Cd or negatively charged (000-1)-Se polar surfaces. This vertical oriented attachment of building primary nanoparticles lead to the formation of thorn-like branches on the surface of rings. As shown in Fig. 5a, this vertical organization can be further confirmed by attachment of new particles at the end of a branch (showed by arrowheads in the A, B and C sections). This behavior is believed to be a consequence of further development of oriented attachment. The connecting region with coherent lattice structure indicated by arrowheads in Fig. 5b (high-magnification HRTEM image of B section in Fig. 5a) powerfully reveal that the building primary crystallites assemble via the "oriented attachment" mechanism.

Type (ii) and type (iii) of organization, which can bring on the birth of hexagonal ring, must be formed with straight segments as a result of the <11-20> and <10-10> directional alignments [30]. So, the quantity of hexagonal rings is less. In this paper, the latter two cases will not be further investigated.

Additionally, lower reaction temperature benefits the anisotropic growth [13, 27]. When the reaction is conducted at higher temperature, the anisotropic growth becomes weaker. Therefore, the branches on the surface of nanocrystals shorten at higher temperature, and even disappear.

The two steps of self-assembly from primary particles to a tribulus-shaped crystal are schematically illustrated in Fig. 5 top. It is generally believed that the synthesis of some nanoparticles often involves the fast nucleation of primary particles and the subsequent growth via their aggregation. The aggregation includes random and oriented aggregation [27]. Firstly, the "core" of tribulus-shaped nanoparticle is formed by the random aggregation of building primary particles. Some facets tending to be the anisotropic growth of wurtzite CdSe nanocrystals [29], which is coming from the primary building blocks, are bared on the surfaces of the "cores". Subsequently, the nomadic building particles attach to these facets with a highly oriented fashion and then produce branches. Figure 5c clearly displays a tribulus-shaped nanoparticle which generated through two steps of attachment. The section A in Fig. 5c contained three random arrangement particles A1, A2, A3, and two oriented attachment branches A4 and A5. Figure 5d, the magnification of section A in Fig. 5c, displays them clearly. Thereinto, the branches A4 and A5 display the <11-20> and <0001> directional attachment, respectively.

Conclusions

In conclusion, a shape-controlled synthesis of CdSe nanorings and tribulus-shaped nanoparticles can be developed without any organic additives at low temperature. The lower reaction temperature benefits the anisotropic growth of crystals with oriented attachment mechanism to produce the high-yield ring- and tribulus-shaped nanocrystals, and produce many branches/arms of products. In photoluminescence spectra, the emission of CdSe nanocrystals synthesized at room temperature has higher blue shift and narrower FWHM than that of products prepared at 60 °C and 100 °C. The structure of tribulus-shaped nanoparticles is achieved via random aggregation and succedent linear oriented aggregation of the building primary particles at room temperature. The nanorings are constructed through a nonlinear arrangement of the building primary particles at lower temperature. This process can provide a new way to fabricate novel architectures. Further investigations are currently under way to identify the underlying mechanism about the hexagonal nanorings growth and to control the size distribution.

Acknowledgments This work was partially supported by the National Nature Science Foundation of China (Grant No.20666005 and 20661003), the Nature Science Foundation of Xinjiang Province (Grant No. 200821121 and 200721102), and The Research Fund for the Doctoral Program of Higher Education (Grant No. 20070755001).

References

1. W.U. Huynh, J.J. Dittmer, A.P. Alivisatos, Science **295**, 2425 (2002). doi:10.1126/science.1069156
2. Y.N. Xia, P.D. Yang, Y.G. Sun, Y.Y. Wu, B. Mayers, B. Gates, Y.D. Yin, F. Kim, Y.Q. Yan, Adv. Mater. **15**, 353 (2003). doi:10.1002/adma.200390087
3. N. Myung, Y. Bae, A.J. Bard, Nano Lett. **3**, 747 (2003). doi:10.1021/nl034165s
4. B.Q. Sun, E. Marx, N.C. Greenham, Nano Lett. **3**, 961 (2003). doi:10.1021/nl0342895
5. W. Luan, H. Yang, N. Fan, S.-T. Tu, Nanoscale Res. Lett. **3**, 134 (2008). doi:10.1007/s11671-008-9125-5
6. M.A. Hahn, P.C. Keng, T.D. Krauss, Anal. Chem. **80**, 864 (2008). doi:10.1021/ac7018365
7. X.G. Peng, L. Manna, W.D. Yang, J. Wickham, E. Scher, A. Kadavanich, A.P. Alivisatos, Nature **404**, 59 (2000). doi:10.1038/35003535
8. Q. Peng, Y. Dong, Z. Deng, Y. Li, Inorg. Chem. **41**, 5249 (2002). doi:10.1021/ic0257266
9. R.F. Li, Z.T. Luo, F. Papadimitrakopoulos, J. Am. Chem. Soc. **128**, 6280 (2006). doi:10.1021/ja058102i
10. F. Shieh, A.E. Saunders, B.A. Korgel, J. Phys. Chem. B **109**, 8538 (2005). doi:10.1021/jp0509008
11. A. Salant, E. Amitay-Sadovsky, U. Banin, J. Am. Chem. Soc. **128**, 10006 (2006). doi:10.1021/ja063192s
12. D.H. Son, S.M. Hughes, Y.D. Yin, A.P. Alivisatos, Science **306**, 1009 (2004). doi:10.1126/science.1103755

13. L. Ouyang, K.N. Maher, C.L. Yu, J. McCarty, H. Park, J. Am. Chem. Soc. **129**, 133 (2007). doi:10.1021/ja066243u
14. Z.Y. Tang, N.A. Kotov, Adv. Mater. **17**, 951 (2005). doi:10.1002/adma.200401593
15. C. Ma, Z.L. Wang, Adv. Mater. **17**, 2635 (2005). doi:10.1002/adma.200500805
16. L.L. Zhao, T.Z. Lu, M. Yosef, M. Steinhart, M. Zacharias, U. Gösele, S. Schlecht, Chem. Mater. **18**, 6094 (2006). doi:10.1021/cm062014v
17. N. Pradhan, H.F. Xu, X.G. Peng, Nano Lett. **6**, 720 (2006). doi:10.1021/nl052497m
18. X.C. Jiang, B. Mayers, T. Herricks, Y.N. Xia, Adv. Mater. **15**, 1740 (2003). doi:10.1002/adma.200305737
19. J. Joo, J.S. Son, S.G. Kwon, J.H. Yu, T. Hyeon, J. Am. Chem. Soc. **128**, 5632 (2006). doi:10.1021/ja0601686
20. J.E. Halpert, V.J. Porter, J.P. Zimmer, M.G. Bawendi, J. Am. Chem. Soc. **128**, 12590 (2006). doi:10.1021/ja0616534
21. L. Manna, E.C. Scher, A.P. Alivisatos, J. Am. Chem. Soc. **122**, 12700 (2000). doi:10.1021/ja003055
22. D. Battaglia, J.J. Li, Y.J. Wang, X.G. Peng, Angew. Chem. Int. Ed. **42**, 5035 (2003). doi:10.1002/anie.200352120
23. G. Zlateva, Z. Zhelev, R. Bakalova, I. Kanno, Inorg. Chem. **46**, 6212 (2007). doi:10.1021/ic062045s
24. L. Liu, Q. Peng, Y. Li, Inorg. Chem. **47**, 3182 (2008). doi:10.1021/ic702203c
25. S.J. Rosenthal, J. McBride, S.J. Pennycook, L.C. Feldman, Surf. Sci. Rep. **62**, 111 (2007). doi:10.1016/j.surfrep.2007.02.001
26. R.L. Penn, J.F. Banfield, Science **281**, 969 (1998). doi:10.1126/science.281.5379.969
27. R.L. Penn, J. Phys. Chem. B **108**, 12707 (2004). doi:10.1021/jp036490
28. Y. Cheng, Y. Wang, D. Chen, F. Bao, J. Phys. Chem. B **109**, 794 (2005). doi:10.1021/jp0460240
29. L. Manna, L.W. Wang, R. Cingolani, A.P. Alivisatos, J. Phys. Chem. B **109**, 6183 (2005). doi:10.1021/jp0445573
30. B. Liu, H.C. Zeng, J. Am. Chem. Soc. **127**, 18262 (2005). doi:10.1021/ja055734w
31. K.-S. Cho, D.V. Talapin, W. Gaschler, C.B. Murray, J. Am. Chem. Soc. **127**, 7140 (2005). doi:10.1021/ja050107s